Kinetics and Mechanisms of the Oxidation of Hydroxylamine by Aqueous Iodine

Rong Ming Liu, Michael R. McDonald, and Dale W. Margerum*

Department of Chemistry, Purdue University, West Lafayette, Indiana 47907

Received June 7, 1995[⊗]

First-order rate constants (k_r, 25.0 °C, μ = 0.50 M) for the loss of I_3^-/I_2 in the presence of excess NH_3OH^+/NH_2OH are measured from pH 2.0 to 6.8 with variation of the reactant concentrations as well as the concentrations of I^- and various buffers. The k_r values range from 5×10^{-4} to 2×10^4 s^{-1} and depend on the NH_2OH concentration. A multistep mechanism is proposed where I_2 and NH_2OH react rapidly to form an I_2NH_2OH adduct ($K_A = 480$ M^{-1}) that undergoes general-base (B) assisted deprotonation to give $INHOH + I^- + BH^+$. At higher pH, hydroxylamine acts as a general base as well as a reductant. Rate constants for various bases (H_2O, CH_3COO^-, NH_2OH, HPO_4^{2-}, and OH^-) fit a Brønsted β value of 0.58. The rates decrease greatly with increases of H^+ and I^- concentrations due to NH_3OH^+ and I_3^- formation, loss of general-base assistance, and the reverse reaction of $BH^+ + I^- + INHOH$ to re-form I_2NH_2OH. The INHOH species is a steady-state intermediate that decays to form $I^- + HNO + H^+$. Subsequent rapid dehydrative dimerization of HNO gives N_2O as the final product. The hydroxylamine oxidation process proceeds entirely by I^+ transfer to nitrogen followed by I^- loss, as opposed to electron-transfer pathways. Kinetic evidence is given for I_2NH_2OH as an intermediate and for INHOH as a steady-state species.

Introduction

Hydroxylamine is used synthetically to form oxime derivatives that are important in the production of pharmaceuticals and polymers. It is also widely used as a reducing agent for photographic processes, dyeing, and other industrial applications.[1,2] In many reactions of hydroxylamine with oxidizing agents the $NH_2O^\bullet$ radical is postulated as an intermediate that can decompose to N_2 or be further oxidized to N_2O. Most of these reactions are with one-electron oxidants.[3] Halogens are two-electron oxidants that react very rapidly with NH_2OH, as shown in recent kinetic studies with chlorine[4] and with bromine.[5] We now compare the reactivity and reaction mechanisms of iodine with the other halogens. We also address the question of whether these oxidations proceed by electron-transfer steps or by halogen cation transfer followed by halide ion elimination.

In the presence of excess hydroxylamine, iodine is rapidly reduced to iodide ion and hydroxylamine is oxidized to nitrous oxide (eq 1). This stoichiometry has been shown to be valid

$$2I_2 + 2NH_2OH \rightarrow N_2O + 4I^- + 4H^+ + H_2O \qquad (1)$$

in weakly basic medium[6] as well as in acidic solutions.[7] Although nitrous acid (HONO) can form in acidic solutions when iodine concentrations exceed the total hydroxylamine concentration, no traces of HONO were found when hydroxylamine was in excess from pH 3.4 to 5.5; N_2O was the only nitrogen product.[8]

The kinetics and mechanisms of the iodine oxidation of hydroxylamine were studied in 1982 by Rábai and Beck,[7] in 1987 by Radhakrishnamurti et al.,[9] and in 1992 by Wang et al.[8] These reports agree that unprotonated hydroxylamine is far more reactive than the protonated species (NH_3OH^+) and that I_2 is much more reactive than triiodide ion, I_3^-. However, these studies disagree with regard to both the magnitude of the rate constants and the mechanisms. Radhakrishnamurti et al.[9] give an impossibly large rate constant of 3.5×10^{11} M^{-1} s^{-1} for the reaction between HOI and NH_2OH. This value is impossible because it is 50 times greater than the diffusion-controlled rate constant ($\sim 7 \times 10^9$ M^{-1} s^{-1}).[10] These authors also suggest an unreasonably small value of 0.4 M^{-1} s^{-1} as the rate constant for the reaction between I_2 and NH_2OH to form an adduct. Iodine reacts extremely rapidly with I^- (5.6×10^9 M^{-1} s^{-1})[11] to form I_3^- and with $S_2O_3^{2-}$ (7.8×10^9 M^{-1} s^{-1})[12] to form the $I_2S_2O_3^{2-}$ adduct. Hence, the corresponding adduct formation between I_2 and NH_2OH cannot be 10 orders of magnitude slower. Finally, they[9] indicate a tendency for the iodine and hydroxylamine reaction to reach a limiting rate at high concentrations of hydroxylamine. Wang et al.[8] show that the $I_2 + NH_2OH$ reaction is much faster, and they find no evidence for a limiting rate up to pH 5.0 with 0.03 M total hydroxylamine ($[NH_2OH]_T = [NH_3OH^+] + [NH_2OH]$).

Radhakrisnamurti et al.[9] suggested an inner-complex mechanism of electron transfer with a pre-equilibrium 1:1 σ-CT interaction between I_2 and NH_2OH. Rábai and Beck[7] suggested NH_2OHI^+ and NH_3OHI^{2+} as reactive intermediates. Wang et al.[8] suggested both a molecular path with $NH_2OI_2^-$ as an intermediate and an electron-transfer path (eq 2), where k_1 =

$$NH_2OH + I_2 \underset{k_{-1}}{\overset{k_1}{\rightleftharpoons}} NH_2O^\bullet + I_2^{\bullet-} + H^+ \qquad K_1 = k_1/k_{-1} \qquad (2)$$

6.5×10^5 M^{-1} s^{-1}. We can rule out this electron-transfer

[⊗] Abstract published in *Advance ACS Abstracts,* November 1, 1995.

(1) *Encyclopedia of Industrial Chemical Analysis*, Wiley: New York, 1971; Vol. 14, p 440.
(2) *Comprehensive Inorganic Chemistry*; Pergamon: New York, 1973; Vol. 2, p 266.
(3) Stedman, G. *Inorganic Chemistry and Radiochemistry*; Academic Press: London, 1979; Vol. 22, pp 122−127.
(4) Cooper, J. N.; Margerum, D. W. *Inorg. Chem.* **1993**, *32*, 5905−5910.
(5) Beckwith, R. C.; Cooper, J. N.; Margerum, D. W. *Inorg. Chem.* **1994**, *33*, 5144−5150.
(6) Bartousek, M. Z. *Anal. Chem.* **1960**, *173*, 193−194.
(7) Rábai, G.; Beck, M. T. *J. Chem. Soc., Dalton Trans.* **1982**, 573−576.
(8) Wang, R. T.; Rábai, G.; Kustin, K. *Int. J. Chem. Kinet.* **1992**, *24*, 11−18.
(9) Radhakrishnamurti, P. S.; Rath, N. K.; Panda, R. K. *Indian J. Chem.* **1987**, *26A*, 412−416.
(10) Caldin, E. F. *Fast Reactions in Solution*; Wiley: London, 1964; pp 10−12.
(11) Ruasse, M.; Aubard, J.; Galland, B.; Adenier, A. *J. Phys. Chem.* **1986**, *90*, 4382−4388.
(12) Scheper, W. M.; Margerum, D. W. *Inorg. Chem.* **1992**, *31*, 5466−5473.

0020-1669/95/1334-6093$09.00/0

pathway on the basis of the extraordinarily low self-exchange rate constant for the NH_2OH^+/NH_2OH couple, where $k_{11} = 5 \times 10^{-13}$ M^{-1} s^{-1}.[13] The $E°$ value for the NH_2OH^+/NH_2OH couple is 0.42 V,[13] the pK_a for NH_2OH^+ is 4.2,[14] and the $E°$ value for the I_2/I_2^- couple is 0.21 V,[14] so the equilibrium constant (K_{12}) for the reaction in eq 3 is 2.8×10^{-4}. A self-

$$NH_2OH + I_2 \overset{k_{12}}{\rightleftharpoons} NH_2OH^+ + I_2^- \quad (3)$$

exchange rate constant for the I_2/I_2^- couple, $k_{22} = 8.5 \times 10^4$ M^{-1} s^{-1}, was estimated in this laboratory,[15] and subsequent work[16] agreed with this value. A recent value of $k_{22} = 4 \times 10^6$ M^{-1} s^{-1} has been reported.[17] On the basis of Marcus theory,[18] where $k_{12} = (k_{11}k_{22}K_{12}f_{12})^{1/2}$ and $\ln f_{12} = \ln(K_{12})^2/4 \ln(k_{11}k_{22}/Z^2)$, the value of k_{12} is calculated to be 2.1×10^{-5} M^{-1} s^{-1} or less. The value suggested by Wang et al.[8] in eq 2 is more than 10 orders of magnitude larger and is clearly too large to permit an electron-transfer mechanism.

In the present work we examine the kinetics of the I_2/I_3^- reaction with NH_2OH/NH_3OH^+ over a pH range (2.0−6.8) wider than was previously used, and we test the effects of buffer and reactant concentrations.

Experimental Section

Reagents. Distilled, deionized water was used for all solutions. Ionic strength (μ) was adjusted to 0.50 M with recrystallized $NaClO_4$. Acidity was adjusted with standardized $HClO_4$ solutions. An Orion Model SA 720 research digital pH meter and a Corning combination electrode were used to measure pH values which were corrected to p[H^+] values at 25.0 °C and $\mu = 0.50$ M based on electrode calibration by titration of standardized $HClO_4$ and NaOH. All chemicals were reagent grade. The concentrations given for kinetic reactions are postmixing values.

Stock solutions of 0.10 M $[I_2]_T$ were prepared by dissolving crystalline I_2 in 0.48 M KI solutions. Stock solutions of 0.200 M NaI were prepared from the crystalline solid and purged with Ar to remove dissolved O_2. These solutions were stored in the dark. Solutions of $NH_2OH·HCl$ (Mallinckrodt) were standardized with $Fe_2(SO_4)_3$, as previously described.[5] Stock solutions of acetic acid (2.0 M) were prepared from dilution of glacial acetic acid, and buffer solutions were prepared by the addition of 1.0 M NaOH. Stock solutions of 0.50 M NaH_2PO_4 were prepared from the crystalline salt, and buffer solutions were made by the addition of 1.0 M NaOH.

The Griess−Ilosvay reaction[7,19,20] was used to test for nitrous acid by reaction with sulfanilic acid followed by a coupling reaction with 1-naphthylamine to give an azo dye ($\lambda_{max} = 520$ nm). A 1% sulfanilic acid solution was prepared by dissolution of the powder in 25% acetic acid. A 0.6% solution of 1-naphthylamine was also prepared in 25% acetic acid.

Negative Tests for HONO/NO_2^- as Products. Since HONO formation and decay was observed in the reactions of Cl_2 and of Br_2 with NH_2OH,[4,5] we tested the stoichiometry given in eq 1 to see if any HONO or NO_2^- formed as a byproduct. At p[H^+] 6.1 with 20 mM $[NH_2OH]_T$, 10 mM [I^-], and 2.0×10^{-5} M $[I_2]_T$, we found no trace ($< 10^{-7}$ M) of NO_2^- after the reaction with iodine. The Griess−Ilsovay reaction was used. Under the same conditions without $[I_2]_T$, a 8.4×10^{-6} M $NaNO_2$ solution gave an absorbance of 0.289 at 520 nm in a 1 cm cell. At pH 6.1 the reaction between NH_3OH^+ and HONO is very slow, as is the reaction between I^- and HONO. Hence, we are confident that HONO does not form at this pH.

Reaction products of $[I_2]_T$, [I^-], and $[NH_2OH]_T$ mixtures were also tested at pH 2−4 and failed to show any evidence of HONO formation. However, at lower pH a proposed[7] I^- catalysis of the reaction between HONO and NH_2OH to give N_2O could interfere. We can only conclude that if any HONO had formed, it reacted further to give N_2O and that the overall stoichiometry in eq 1 appears to be valid.

Kinetic Measurements. All reactions were followed by the loss of I_3^- absorbance at 353 nm ($\epsilon_{I_3} = 26\,400$ M^{-1} cm^{-1})[21] in the presence of excess I^- and excess total hydroxylamine. Excellent pseudo-first-order rates were observed in accord with eq 4, where $[I_2]_T = [I_3^-] + [I_2]$ and k_r is a function of the concentrations of $[NH_2OH]_T$, [I^-], [H^+], and buffer concentrations.

$$-d[I_2]_T/dt = k_r[I_2]_T \quad (4)$$

Slower reactions at low pH (half-lives of 36 s to 36 min) were measured with a Perkin-Elmer Lambda-9 UV/vis/near-IR spectrophotometer interfaced to a Zenith 386/20 computer. Reactions in acetic acid/acetate buffer with half-lives of 3 ms to 1 s were monitored by stopped-flow methods by using computer interfaced Durrum or Hi-Tech instruments.[5] Faster reactions (above pH 5) with NH_3OH^+/NH_2OH or $H_2PO_4^-/HPO_4^{2-}$ as buffers were measured by pulsed-accelerated-flow (PAF) methods.[22−26] Solutions for all PAF experiments were filtered and degassed.

PAF Method with Integrating Observation. The PAF Model IV spectrophotometer[24,25] and previous PAF instruments have used integrating observation during continuous accelerated flow mixing of short duration. The light path is along the direction of flow. The measured rate constant depends on the initial absorbance of the reactants, A_0, the absorbance at a given instantaneous velocity, A_v, and the final absorbance, A_∞. Pseudo-first-order rate constants, k_r, can be determined by using eq 5, where b is the reaction path length (0.010 25 m), v is

$$M_{exptl} = \frac{A_v - A_\infty}{A_0 - A_\infty} = \frac{1}{bk_m} + \frac{v}{bk_r} \quad (5)$$

the solution velocity (12 to 3 m/s), and k_m is a proportionality constant from the mixing rate constant ($k_{mix} = k_m v$). In the PAF integrating observation technique, the reactants are observed from the point where they initially mix until they exit the observation tube. The method is capable of measuring fast reactions with half-lives in the range of 4 μs to 1 ms. However, this PAF method requires knowledge of A_0. An extremely fast reaction that decreases A_0 prior to the reaction under study will give observed k_r values that are too large. This problem can be overcome by use of the PAF−PRO instrument in which observation is made across the flow rather than by integrated observation along the direction of flow.

Pulsed-Accelerated Flow with Position-Resolved Observation. A new pulsed-accelerated-flow spectrometer with position-resolved observation (PAF−PRO) has been developed in this laboratory.[26] The instrument utilizes a wider range of velocities than the PAF-IV instrument, and observation is perpendicular to solution flow at multiple points in the observation tube. A masked charge-coupled device (CCD) with 1024 × 1024 resolution elements in an 8 × 8 binning mode enables observation at 128 discrete positions along the observation tube (1.945 cm in length). The progress of the reaction is monitored as a function of the distance the solution travels down the observation tube at 126

(13) Hung, M.-L.; McKee, M. L.; Stanbury, D. M. *Inorg. Chem.* **1994**, *33*, 5108−5112.
(14) Stanbury, D. M. *Adv. Inorg. Chem.* **1989**, *33*, 69−133.
(15) Woodruff, W. H.; Margerum, D. W. *Inorg. Chem.* **1974**, *13*, 2578−2585.
(16) Ishikawa, K.; Jukuzumi, S.; Tanaka, T. *Inorg. Chem.* **1989**, *28*, 1661−1665.
(17) Shi, S.; Espenson, J. H.; Meyerstein, D.; Meisel, D. *Inorg. Chem.* **1991**, *30*, 4468−4470.
(18) Marcus, R. A. *J. Chem. Phys.* **1965**, *43*, 679−701.
(19) Tomlinson, G.; Cruickshank, W. H.; Viswantha, T. *Anal. Biochem.* **1971**, *44*, 670−679.
(20) Blom, J. *Ber. Dtsch. Chem. Ges.* **1926**, *59*, 121.
(21) Awtrey, A. D.; Connick, R. E. *J. Am. Chem. Soc.* **1951**, *73*, 1341−1348.
(22) Jacobs, S. A.; Nemeth, M. T.; Kramer, G. W.; Ridley, T. Y.; Margerum, D. W. *Anal. Chem.* **1984**, *56*, 1058−1065.
(23) Nemeth, M. T.; Fogelman, K. D.; Ridley, T. Y.; Margerum, D. W. *Anal. Chem.* **1987**, *59*, 283−291.
(24) Fogelman, K. D.; Walker, D. M.; Margerum, D. W. *Inorg. Chem.* **1989**, *28*, 986−993.
(25) Bowers, C. P.; Fogelman, K. D.; Nagy, J. C.; Ridley, T. Y.; Wang, Y. L.; Evetts, S. W.; Margerum, D. W. To be submitted for publication.
(26) McDonald, M. R.; Wang, T. X.; Gazda, M.; Scheper, W. M.; Evetts, S. W.; Margerum, D. W. To be submitted for publication.

different flow velocities in the range of 19.7 to 2.2 m/s. Data for a single kinetic run are collected in 0.5 s with the consumption of 11.0 mL of each reagent. Since observation is perpendicular to solution flow, the optical path length is determined by the width of the observation tube (0.212 cm). Reaction half-lives can be measured in the range of 0.07−3 ms.

For pseudo-first-order reactions, the absorbance (A_p) is measured at 128 positions along the observation cell, and these positions are converted to the appropriate time scale for each flow velocity. The apparent rate constant, k_{app}, is evaluated from plots of $\ln(A_p - A_\infty)$ vs time for each of 126 different flow velocities. On the basis of earlier studies,[22,23] the physical mixing rate constant is proportional to the flow velocity ($k_{mix} = k_m v$), and eq 6 relates the apparent rate constant to the chemical reaction rate constant (k_r) and the mixing rate constant. A double reciprocal plot of $1/k_{app}$ against $1/v$ gives $1/k_r$ as the intercept.

$$\frac{1}{k_{app}} = \frac{1}{k_m}\left(\frac{1}{v}\right) + \frac{1}{k_r} \qquad (6)$$

Results and Discussion

Rate constants for the loss of $[I_2]_T$ are measured with variation of $[NH_2OH]_T$, $[I^-]$, $[H^+]$, and buffer concentrations. While we agree with earlier results that indicate the reactive species are I_2 and NH_2OH, rather than I_3^- or NH_3OH^+, we observe four aspects of these reactions that had not been reported previously. (1) The reactions are general-base assisted, where CH_3COO^-, NH_2OH, HPO_4^{2-}, and OH^- accelerate the rate of loss of iodine. At high concentrations of hydroxylamine, the rate expression contains both $[NH_2OH]$ and $[NH_2OH]^2$ terms, because hydroxylamine acts as a nucleophile and as a general base. (2) Kinetic evidence is obtained for appreciable concentrations of a hydroxylamine−iodine adduct, I_2NH_2OH. (3) Kinetic evidence is found for INHOH as a steady-state species. (4) At low pH the rate is suppressed by $[H^+]$ to a greater extent than can be attributed to NH_3OH^+ formation. We also confirm an earlier observation[7] that at low pH the rate is suppressed by $[I^-]$ concentration to a greater extent than can be attributed to I_3^- formation. The rate dependencies are moderately complicated, so we shall take the liberty of presenting all the steps in the proposed mechanism (eqs 7−13) before we show how it

Proposed Mechanism

$$I_2 + I^- \overset{K_I}{\rightleftharpoons} I_3^- \qquad (7)$$

$$NH_2OH + H^+ \overset{K_P}{\rightleftharpoons} NH_3OH^+ \qquad (8)$$

$$I_2 + NH_2OH \underset{k_{-a}}{\overset{k_a}{\rightleftharpoons}} I_2NH_2OH \qquad (9)$$

$$I_2NH_2OH \underset{k_{-b}}{\overset{k_b}{\rightleftharpoons}} I^- + INHOH + H^+ \qquad (10)$$

$$I_2NH_2OH + B \underset{k_{-B}}{\overset{k_B}{\rightleftharpoons}} I^- + INHOH + HB^+ \qquad (11)$$

$$INHOH \xrightarrow{k_c} I^- + HNO + H^+ \qquad (12)$$

$$2HNO \xrightarrow[\text{rapid}]{k_d} N_2O + H_2O \qquad (13)$$

accounts for the results. At 25.0 °C and $\mu = 0.50$ M, the value for K_I is 721 M^{-1} [27] and the value for K_p is 1.01×10^6 M^{-1}.[28] The rate constant for I_3^- formation[11] in eq 7 is 5.6×10^9 M^{-1} s^{-1}, and the protonation rate constant to give NH_3OH^+ should be greater than 10^{10} M^{-1} s^{-1},[29] so reactions 7 and 8 are in rapid equilibria. The dehydrative dimerization reaction in eq 13 is very fast; the value for k_d is reported to be $(4.5 \pm 2.7) \times 10^9$ M^{-1} s^{-1}.[30] If we assume that reaction 9 is in rapid equilibrium and treat INHOH as a steady-state species, the rate expression in eq 14 is obtained (where $K_A = k_a/k_{-a}$). If $K_a^{HB} = [H^+][B]/[HB^+]$, it can be shown that $k_{-B} = k_{-b}K_a^{HB}k_B/k_b$, and this substitution in eq 14 gives eq 15. This mechanism assumes that since the electron pair on the hydroxylamine nitrogen is the strongest Lewis base in the molecule, it will be used to form an I_2NH_2OH complex rather than the electron pair on oxygen, as implied by others.[7,8] Primary, secondary, and tertiary amines form adducts with iodine in *n*-heptane solutions.[31,32] A crystal structure has been determined for $(CH_3)_3NI_2$.[33] As mentioned previously, the rate of I_2 adduct formation is extremely rapid, so we expect k_a to be near the diffusion-limiting value of 7×10^9 M^{-1} s^{-1}.[10] The rate-determining steps in the proposed mechanism are attributed to the formation and decay of INHOH.

$$k_r = (k_b + \sum k_B[B])[NH_2OH]_T K_A k_c/(1 + K_P[H^+])(1 + K_I[I^-])(k_{-b}[I^-][H^+] + \sum k_{-B}[I^-][HB^+] + k_c) \qquad (14)$$

$$k_r = (k_b + \sum k_B[B])[NH_2OH]_T K_A/(1 + K_P[H^+])(1 + K_I[I^-])\left(\frac{k_{-b}}{k_c}[I^-][H^+]\left(1 + \frac{\sum k_B[B]}{k_b}\right) + 1\right) \qquad (15)$$

Kinetics at Low pH without Added Buffers. The rate of loss of iodine in 9.90 mM $[H^+]$ is relatively slow, and the rate constants decrease markedly as the I^- concentration increases (Table 1). Under these conditions, the general-base catalyzed pathway should be negligible and the $\sum k_B[B]$ term can be deleted from eq 15. This leads to eq 16 as the expression for

$$k_r = k_b K_A [NH_2OH]_T/(1 + K_p[H^+])(1 + K_I[I^-])\left(\frac{k_{-b}}{k_c}[I^-][H^+] + 1\right) \qquad (16)$$

Table 1. Effect of Hydrogen Ion and Iodide Ion Concentrations on the Observed Rate Constant at Low pH without Added Buffers[a]

$[H^+]$, mM	$[NH_2OH]_T$, mM	$[I^-]$, mM	$10^3 k_r$, s^{-1}
1.15	5.023	10.0	19.2
2.88	5.023	10.0	5.66
5.77	10.05	10.0	4.31
7.21	5.023	10.0	1.65
7.21	5.023	20.0	0.555
9.90	5.019	3.00	5.69
9.90	5.019	5.00	3.12
9.90	5.019	8.00	1.83
9.90	5.019	10.0	1.28
9.90	5.019	13.0	0.837
9.90	5.019	15.0	0.590
9.90	5.019	18.0	0.509
9.90	5.019	23.0	0.321

[a] Conditions: 25.0 ± 0.1 °C; $[I_2]_T = 2.1 \times 10^{-5}$ M; $\mu = 0.50$ M ($NaClO_4$); rate constants are evaluated from single runs.

(27) Ramette, R. W.; Sandford, R. W. *J. Am. Chem. Soc.* **1965**, *87*, 5001−5005.
(28) Lumme, P.; Lahermo, P.; Tummavuori, J. *Acta Chem. Scand.* **1965**, *19*, 2175−2188.
(29) Eigen, M. *Angew. Chem., Int. Ed. Engl.* **1964**, *3*, 1−19.
(30) Bazylinski, D. A.; Hollocher, T. C. *Inorg. Chem.* **1985**, *24*, 4285−4288.
(31) Drago, R. S.; Meek, D. W.; Longhi, R.; Joesten, M. D. *Inorg. Chem.* **1963**, *2*, 1056−1060.
(32) Yada, H.; Tanaka, J.; Nagakura, S. *Bull. Chem. Soc. Jpn.* **1960**, *33*, 1660−1667.
(33) Strømme, K. O. *Acta Chem. Scand.* **1959**, *13*, 268−274.

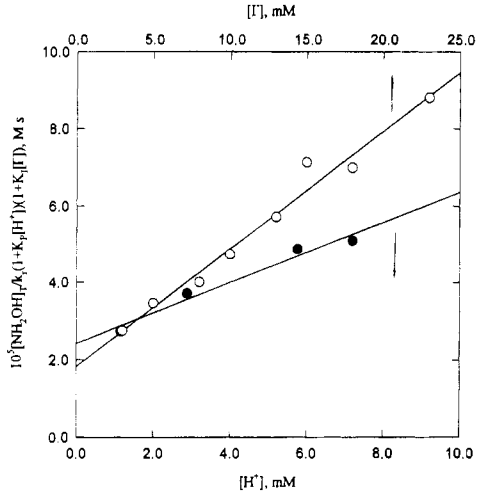

Figure 1. Top abcissa: Dependence of the reciprocal of the observed rate constant in 9.9 mM $[H^+]$ (corrected for the formation of NH_3OH^+ and I_3^-), on $[I^-]$ (eq 17). The positive slope indicates additional suppression of the rate by I^- and gives $k_{-b}/k_c = (1.7 \pm 0.3) \times 10^4$ M^{-2} and $k_bK_A = (5.5 \pm 1.1) \times 10^4$ M^{-1} s^{-1}. Bottom abcissa: Dependence on $[H^+]$ at constant $[I^-]$ (10.0 mM). The positive slope indicates added suppression by $[H^+]$ and gives $k_{-b}/k_c = (1.6 \pm 0.1) \times 10^4$ M^{-2} and $k_bK_A = (4.1 \pm 0.3) \times 10^4$ M^{-1} s^{-1}.

the observed first-order rate constant. Rearrangement of eq 16 gives eq 17, and the left-hand side is plotted against $[I^-]$ in

$$\frac{[NH_2OH]_T}{k_r(1 + K_p[H^+])(1 + K_I[I^-])} = \frac{k_{-b}}{k_bK_Ak_c}[I^-][H^+] + \frac{1}{k_bK_A} \quad (17)$$

Figure 1. Since the values of the ordinate are already corrected for suppression of the rate by I_3^- and NH_3OH^+, a horizontal line would be expected from previously proposed mechanisms.[7,8] However, the ordinate values (proportional to the reciprocal of k_r) increase as $[I^-]$ increases, which indicates that there is an additional source of I^- suppression of the reaction rate. We attribute this suppression to the reversibility of INHOH formation in eq 10 of the mechanism. These data give $k_bK_A = (5.5 \pm 1.1) \times 10^4$ M^{-1} s^{-1} and $k_{-b}/k_c = (1.7 \pm 0.3) \times 10^4$ M^{-2}.

Data in Table 1 also show that at low pH the k_r values decrease markedly as the $[H^+]$ concentration increases. The effect is greater than can be attributed to the NH_3OH^+/NH_2OH equilibrium. Figure 1 shows a plot of the left-hand side of eq 17 against the $[H^+]$ at constant $[I^-]$. These data give $k_bK_A = (4.1 \pm 0.3) \times 10^4$ M^{-1} s^{-1} and $k_{-b}/k_c = (1.6 \pm 0.1) \times 10^4$ M^{-2}. The additional suppression is again attributed to the reversibility of INHOH formation in eq 10. We consider the value of the intercept obtained from the $[I^-]$ dependence in Figure 1 to be more reliable.

Kinetics at pH 6 or Greater with Excess Hydroxylamine as a Buffer. Under these conditions the rate of loss of I_3^-/I_2 is too fast to measure by stopped-flow methods. Although the reactions are easily observed by the PAF method with integrating observation, we find that the apparent rate constants evaluated by eq 5 are not self-consistent as the concentration of NH_2OH and the pH are varied. In this equation, A_0 is calculated for the postmixed I_3^-/I_2 solution before it reacts with NH_2OH. If an extremely fast reaction occurs between I_2 and NH_2OH to form I_2NH_2OH (as proposed in eq 9), the initial absorbance prior to the measured reaction may be significantly less than the assigned value because some I_3^- is instantaneously converted to I_2NH_2OH. As a consequence, the k_r value calculated from eq 5 will be too large. This error is inherent in the integrating observation method, because the calculations are based on a single step process for observable reactants and products. (This PAF method can evaluate multistep mechanisms if the intermediates do not have appreciable concentrations or if additional information permits corrected values for A_0.)

Table 2. Hydroxylamine and Hydroxide Ion Dependence Measured on the PAF–PRO[a]

$[NH_2OH]_T$, mM	p$[H^+]$	$10^{-3}k_r$,[b] s^{-1}	$[NH_2OH]_T$, mM	p$[H^+]$	$10^{-3}k_r$,[b] s^{-1}
10.12	6.00	0.618 ± 0.003	50.61	6.06	9.6 ± 0.1
15.18	6.03	1.13 ± 0.02	20.00	6.21	2.92 ± 0.06
20.00	6.07	2.27 ± 0.02	20.00	6.34	3.6 ± 0.1
25.31	6.04	2.88 ± 0.05	20.00	6.48	4.14 ± 0.08
30.37	6.04	3.86 ± 0.07	20.00	6.63	4.89 ± 0.08
40.49	6.05	6.02 ± 0.04	20.00	6.84	5.7 ± 0.2

[a] Conditions: 25.0 ± 0.1 °C; $\mu = 0.50$ M ($NaClO_4$); $\lambda = 353$ nm; $[I^-] = 20$ mM; $[I_2]_T = 0.2$ mM. [b] The k_r values (average of four to five trials) are obtained from the double reciprocal relationship in eq 8, where k_{app} is the apparent first-order rate constant for the loss of I_3^-.

The new PAF–PRO instrument avoids this problem. The progress of the reaction is observed perpendicular to the direction of flow, and the loss of absorbance of I_3^- is measured as the reaction mixture moves along the observation cell. Extremely fast reactions between I_2 and NH_2OH to form appreciable amounts of I_2NH_2OH decrease the A_p values due to the initial I_3^- loss but do not otherwise affect the pseudo-first-order k_{app} values in the subsequent reactions. The k_{app} values are independent of A_0.

Table 2 shows that values of k_r increase from 618 to 9600 s^{-1} as the $[NH_2OH]_T$ increases from 10.1 to 50.6 mM at p$[H^+]$ = 6.03 ± 0.03. Table 2 also gives the dependence of k_r as the p$[H^+]$ values increase from 6.07 to 6.84 at constant $[NH_2OH]_T$. The absorbance changes measured with the PAF–PRO instrument indicate that appreciable amounts of I_2NH_2OH are formed prior to the observed reaction. The definition of $[I_2]_T$ under these conditions is given by eq 18, where $[I_2NH_2OH] =$

$$[I_2]_T = [I_2] + [I_3^-] + [I_2NH_2OH] \quad (18)$$

$K_A[NH_2OH][I_2]$. (Since $NH_2OH{\cdot}HCl$ was used, we also considered I_2Cl^- formation. However, its association constant is only 1.7 M^{-1},[34] and the amount of I_2Cl^- present is negligible.) The rate expression in eq 15 can now be written in terms of eq 19, where the rate-determining step is the breakup of I_2NH_2-

$$\frac{k_r(1 + K_p[H^+])(1 + K_I[I^-] + K_A[NH_2OH])}{[NH_2OH]_T} = (k_b + k_{NH_2OH}[NH_2OH] + k_{OH}[OH^-])K_A \quad (19)$$

OH (eqs 10 and 11) with negligible reversibility for these steps in the mechanisms at higher pH (i.e., $(k_{-b}/k_c)[I^-][H^+] \ll 1$). Data in Table 2 were analyzed with a nonlinear Marquardt–Levenberg algorithm[35] to calculate the best fit of the rate constants (k_{NH_2OH} and k_{OH}) and the equilibrium constant (K_A) to the relationship in eq 19, where a value of 5.5×10^4 M^{-1} s^{-1} for k_bK_A determined from the low pH data is used. The nonlinear fit yields the values of $k_{NH_2OH} = (7.3 \pm 1.2) \times 10^5$ M^{-1} s^{-1}, $k_{OH} = (1.9 \pm 0.7) \times 10^{10}$ M^{-1} s^{-1}, and $K_A = k_a/k_{-a} = (4.8 \pm 1.3) \times 10^2$ M^{-1}. These values are further confirmed by the linear fit illustrated in Figure 2, which shows

(34) Cason, D. L.; Neumann, H. M. *J. Am. Chem. Soc.* **1961**, *83*, 1822–1828.
(35) Sigma Plot, revision spw 1.02 July 1993, Jandel Scientific, San Rafael, CA.

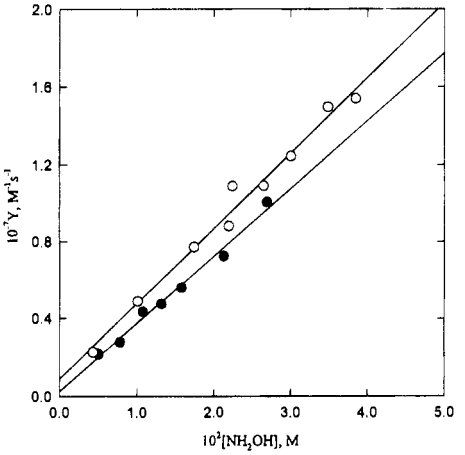

Figure 2. PAF−PRO and PAF-IV data at p[H$^+$] 6.03 ± 0.03 for the pseudo-first-order rate constants for the loss of $[I_2]_T$ as a function of excess $[NH_2OH]$. The Y values are defined by the left-hand side of eq 19 where K_A = 480 M^{-1}: ●, PAF-PRO data; ○, PAF-IV data after correction of A_0 based on K_A. The slope for the PAF−PRO data corresponds to $k_{NH_2OH}K_A$ and gives a k_{NH_2OH} value of 7.3 × 10^5 M^{-1} s^{-1}.

a plot of the left-hand side of eq 19 (defined as Y) against the free NH_2OH concentration at constant p[H$^+$] = 6.03. The positive slope corresponds to contributions of $[NH_2OH]^2$ to the overall rate, because hydroxylamine acts as both a nucleophile and a general base. The slope is 3.5 × 10^8 M^{-2} s^{-1} = $k_{NH_2OH}K_A$, and the intercept is 2.5 × 10^5 M^{-1} s^{-1} = (k_b + k_{OH}[OH$^-$])K_A. This gives k_{NH_2OH} = 7.3 × 10^5 M^{-1} s^{-1}, k_b = 115 s^{-1} (from the evaluation of k_bK_A at low pH), and k_{OH} = 2.0 × 10^{10} M^{-1} s^{-1}. Data in Table 2 at constant $[NH_2OH]_T$ and variable p[H$^+$] permit a value of 1.9 × 10^{10} M^{-1} s^{-1} to be calculated for k_{OH}. Despite the relatively small contribution of the k_{OH}[OH$^-$]K_A term to the observed rate constant, there is good agreement between the k_{OH} values from the intercept in Figure 2 and these data. It is difficult to use higher pH conditions for additional tests of the rate expression because of the lack of buffer capacity, the hydrolysis of I_2, and the extremely fast reactions. Proton-transfer rate constants to OH$^-$ often exceed the diffusion limiting value due to hydrogen bonding, and values of (1−4) × 10^{10} M^{-1} s^{-1} have been measured[29] for many weak acids.

Once the K_A value is known, it is possible to correct the A_0 values used for the PAF-IV calculations. (The absorbance contribution of I_2NH_2OH is assumed to be negligible compared to the absorbance of I_3^- at 353 nm, as is the case for I_2(aq) and $I_2S_2O_3^{2-}$.[12]) Although the corrections are large, Figure 2 shows that the corrected PAF-IV data give a slope of 3.9 × 10^8 M^{-2} s^{-1}, which is in reasonable agreement with the value of 3.5 × 10^8 M^{-2} s^{-1} obtained from the PAF−PRO experiments. We consider the PAF−PRO values to be more accurate; however, it is important to show the validity of this type of correction.

Kinetics with Phosphate Buffer. We found no evidence for a $(I_2OPO_3H)^{2-}$ complex based on the lack of absorbance changes at 353 nm for a 4.8 × 10^{-5} M $[I_2]_T$ solution in 20 mM I$^-$ and 200 mM total phosphate buffer concentration ($[PO_4]_T$ = $[H_2PO_4^-]$ + $[HPO_4^{2-}]$) at p[H$^+$] 6.71. The PAF-IV method was used to study reactions with variation of the $[PO_4]_T$ concentration from 12.5 to 188 mM at p[H$^+$] 5.8 to 6.5 and with $[NH_2OH]_T$ concentrations of 2.5 and 10.0 mM, [I$^-$] = 10 mM, and $[I_2]_T$ = 2.1 × 10^{-5} M. The results given in Table 3 show that the corrections necessitated by A_0 changes (due to I_2NH_2OH formation) result in only a 10−30% decrease of the k_r values. The k_r^{corr} values are reliable rate constants for the phosphate catalyzed reactions, and the results are shown in Figure 3 where Y'_{corr} is given by eq 20 with K_A = 480 M^{-1}.

Table 3. Phosphate Dependence Measured with the PAF-IV[a]

$[PO_4]_T$,[b] mM	p[H$^+$]	$[NH_2OH]_T$, mM	$10^{-3}k_r$,[c] s^{-1}	$10^{-3}k_r^{corr}$,[d] s^{-1}
12.50	5.82	10.05	1.70	1.38
25.00	6.08	10.05	4.18	3.17
50.00	6.28	10.05	11.7	8.45
62.50	6.35	10.05	14.9	10.6
71.25	6.46	2.513	4.48	4.04
77.50	6.44	2.513	4.92	4.44
81.25	6.45	2.513	5.07	4.58
83.75	6.47	2.513	5.24	4.72
125.0	6.41	2.513	6.69	6.05
150.0	6.46	2.513	8.18	7.38
168.8	6.48	2.513	7.51	6.77
187.5	6.53	2.513	9.91	8.90

[a] Conditions: 25.0 ± 0.1 °C; μ = 0.50 M ($NaClO_4$); λ = 353 nm; [I$^-$] = 0.010 M; $[I_2]_T$ = 2.1 × 10^{-5} M. [b] $[PO_4]_T$ = $[HPO_4^{2-}]$ + $[H_2PO_4^-]$. [c] k_r values (four to five trials) measured from PAF-IV prior to the corrections for the decrease of A_0. [d] k_r^{corr} = k_r × 8.21/(8.21 + K_A[NH_2OH]), where K_A = 480 M^{-1}.

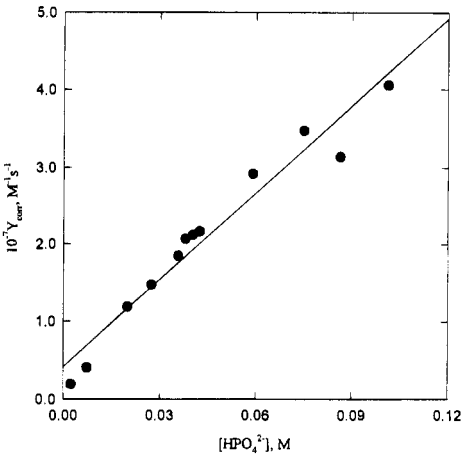

Figure 3. Hydrogen phosphate ion catalysis of the reaction between I_2 and NH_2OH measured by the PAF-IV method with correction of A_0 based on K_A = 480 M^{-1}. The Y'_{corr} value is given by eq 20. The slope equals $k_{HPO_4}K_A$ and corresponds to a k_{HPO_4} value of 7.7 × 10^5 M^{-1} s^{-1}.

The slope, which corresponds to $k_{HPO_4}K_A$ (eq 21), equals 3.7 ×

$$Y'_{corr} = \frac{k_r^{corr}(1 + K_p[H^+])(1 + K_I[I^-] + K_A[NH_2OH])}{[NH_2OH]_T} - k_{OH}K_A[OH^-] - k_{NH_2OH}K_A[NH_2OH] \quad (20)$$

$$Y'_{corr} = k_{HPO_4}K_A[HPO_4^{2-}] + k_bK_A \quad (21)$$

10^8 M^{-2} s^{-1}; therefore, k_{HPO_4} = 7.7 × 10^5 M^{-1} s^{-1}. It should be noted that the values for k_{NH_2OH} and k_{HPO_4} are similar, as expected for general-base catalysis by bases of similar strength.

Kinetics with Acetate Buffer. Stopped-flow methods (Table 4) are used to measure the reaction rates from p[H$^+$] 3.4 to 5.0 in 0.20 M total acetate ($[HOAc]_T$ = [OAc$^-$] + [HOAc]), with 10 mM $[NH_2OH]_T$, 10 mM [I$^-$], and 2.1 × 10^{-5} M $[I_2]_T$. The k_r values are dependent on the [H$^+$] concentration as well as the acetate concentration, and all the mechanistic steps in eqs 7−13 must now be considered. If Y is defined by the left-hand side of eq 19, its dependence is given by eq 22, where B

$$Y = (k_b + \sum k_B[B])K_A/\left[\frac{k_{-b}}{k_c}[I^-][H^+]\left(1 + \frac{\sum k_B[B]}{k_b}\right) + 1\right] \quad (22)$$

is OAc$^-$, NH_2OH, and OH$^-$. The value of k_{OAC} (2.3 × 10^4

Table 4. p[H$^+$] Dependence in Acetate Buffer Measured by Stopped-Flow Methods[a]

p[H$^+$]	[NH_2OH]$_T$, mM	k_r,[b] s^{-1}	p[H$^+$]	[NH_2OH]$_T$, mM	k_r,[b] s^{-1}
3.44	10.13	0.851 ± 0.008	4.49	9.802	40.9 ± 0.4
3.67	10.13	2.22 ± 0.002	4.57	9.802	53.8 ± 0.7
3.82	10.13	3.89 ± 0.13	4.66	9.802	71.9 ± 0.7
4.00	10.13	8.22 ± 0.11	4.76	9.802	99 ± 1
4.18	10.13	16.2 ± 0.4	4.87	9.802	139 ± 3
4.27	10.13	23.1 ± 0.3	4.98	9.802	196 ± 6

[a] Conditions: 25.0 ± 0.1 °C; μ = 0.50 M ($NaClO_4$); λ = 353 nm; [I$^-$] = 0.010 M; $[I_2]_T = 2.1 \times 10^{-5}$ M; $[HOAc]_T$ = 0.20 M. [b] Experimental stopped-flow rate constants (k_{expt}) larger than 50 s^{-1} were corrected for mixing limitations of the instruments by using $k_r = k_{expt}/(1 - (k_{expt}/k_{mix}))$, where k_{mix} = 2900 s^{-1} for the Hi-Tech and k_{mix} = 5276 s^{-1} for the Durrum.

Table 5. Summary of Equilibrium and Rate Constants[a]

constant	value	constant	value
K_I	721 M^{-1} [b]	k_{NH_2OH}	(7.3 ± 1.2) × 10^5 M^{-1} s^{-1}
K_p	1.01 × 10^6 M^{-1} [c]	k_{HPO_4}	(7.7 ± 0.4) × 10^5 M^{-1} s^{-1}
K_A	(4.8 ± 1.3) × 10^2 M^{-1}	k_{OH}	(1.9 ± 0.7) × 10^{10} M^{-1} s^{-1}
k_a	~7 × 10^9 M^{-1} s^{-1}	k_{-b}/k_c	(1.7 ± 0.2) × 10^4 M^{-2}
k_b	(1.15 ± 0.23) × 10^2 s^{-1}	k_d	~5 × 10^9 M^{-1} s^{-1} [d]
k_{OAc}	(2.3 ± 0.1) × 10^4 M^{-1} s^{-1}		

[a] Conditions: 25.0 °C; μ = 0.50 M. [b] Reference 27. [c] Reference 28. [d] Reference 30.

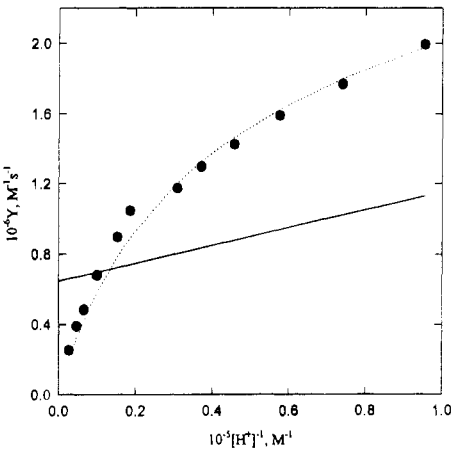

Figure 4. Stopped-flow data for the rate dependence on 1/[H$^+$] in acetate buffer, where the experimental points for k_r are converted to Y as defined by the left-hand side of eq 19, and the dashed line shows the fit of Y to eq 22. This gives a rate constant of 2.3 × 10^4 M^{-1} s^{-1} for the acetate ion reaction with I_2NH_2OH. The solid line shows the failure of the predicted dependence given in ref 8, where the ordinate is $k_r(1 + K_p[H^+])(1 + K_I[I^-])/[NH_2OH]_T$.

M^{-1} s^{-1}) was determined from the fit[35] of the data (Table 4) to eq 22, where K_A = 480 M^{-1}, k_b = 115 s^{-1}, $k_{-b}/k_c = 1.7 \times 10^4$ M^{-2}, $k_{NH_2OH} = 7.3 \times 10^5$ M^{-1} s^{-1}, and $k_{OH} = 1.9 \times 10^{10}$ M^{-1} s^{-1}. Figure 4 shows the fit of the Y term plotted against 1/[H$^+$]. The dependence predicted from the paper by Wang et al.[8] is shown for comparison. They were not aware that acetate ion assisted the rate and that there was additional suppression by [I$^-$] and [H$^+$].

Rejection of Another General-Base-Assisted Mechanism. An alternative mechanism was considered in which base-assisted decomposition of INHOH occurs (eq 23) rather than the

$$INHOH + B \xrightarrow{k_c^B} I^- + HNO + HB^+ \qquad (23)$$

corresponding reaction of I_2NH_2OH as proposed in eq 11. At low pH without added buffers, the alternative mechanism gives exactly the same expression for k_r found in eq 16. At high pH and high buffer concentrations, the Y term (defined by the left-hand side of eq 19) would now be expressed by eq 24. Since $(k_{-b}/k_c)[I^-][H^+] \ll 1 + (k_c^B[B]/k_c)$, it follows that $Y = k_bK_A$ and there would be no general-base assistance. Therefore, the alternative mechanism is not suitable.

Table 6. Brønsted–Pedersen Relationship[a]

B	pK_a(HB$^+$)	p[b]	q[c]	log(k_B/q)	log(p/qK_a)
H_2O	−1.73[a]	3	2	0.021	−1.55
OAc^-	4.41[d]	1	2	4.06	4.11
NH_2OH	6.0[e]	3	1	5.86	6.48
HPO_4^{2-}	6.46[f]	2	3	5.41	6.28
OH^-	15.34[g]	2	3	9.80	15.16

[a] Reference 36. [b] p is the number of equivalent proton sites on HB$^+$. [c] q is the number of equivalent basic sites on B. [d] Reference 40. [e] Reference 28. [f] Reference 41. [g] Reference 42.

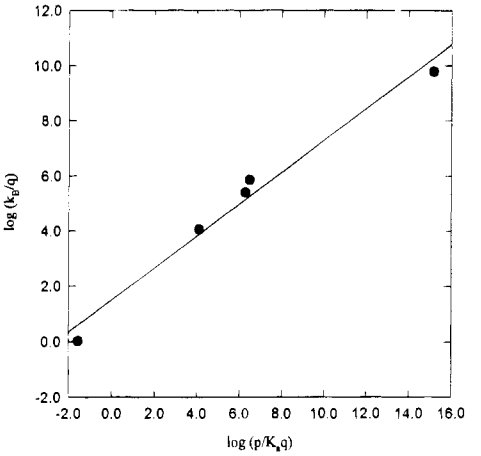

Figure 5. Brønsted–Pedersen plot of the rate constants for the general-base-assisted proton-transfer reactions with I_2NH_2OH. The slope (β) is 0.58.

Scheme 1

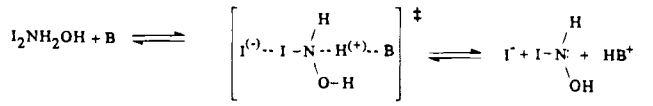

$$Y = \left(1 + \frac{\sum k_c^B[B]}{k_c}\right) k_b K_A \Big/ \left[\frac{k_{-b}}{k_c}[I^-][H^+] + 1 + \frac{\sum k_c^B[B]}{k_c}\right] \qquad (24)$$

Brønsted–Pedersen Relationship. Table 6 summarizes the pK_a values for HB$^+$ and shows the statistical corrections used for the Brønsted–Pedersen plot[36] in Figure 5. The k_B value for H_2O equals $k_b/55.5$ = 2.1 M^{-1} s^{-1}. (Other k_B values are given in Table 5.) The slope for this plot gives β = 0.58; this indicates a transition state shown in Scheme 1 in which there is a significant degree of proton transfer from I_2NH_2OH to B as I$^-$ leaves to give HB$^+$ + INHOH + I$^-$.

Adducts of I_2 with Nucleophiles. Stability constants (K_f) for adduct formation between I_2(aq) and various nucleophiles increase greatly with an increase in the nucleophilicity of the Lewis bases.[12] Figure 6 shows the correlation of log K_f values with the values for the n_{CH_3I} nucleophilic reactivity constants.[37] A n_{CH_3I} value of 6.60 is reported[37] for NH_2OH, and we use our

(36) Bell, R. P. *The Proton in Chemistry*, 2nd ed.; Cornell University Press: Ithaca, NY, 1973; p 198.
(37) Pearson, R. G.; Sobel, H.; Songstad, J. *J. Am. Chem. Soc.* **1968**, *90*, 319–326.

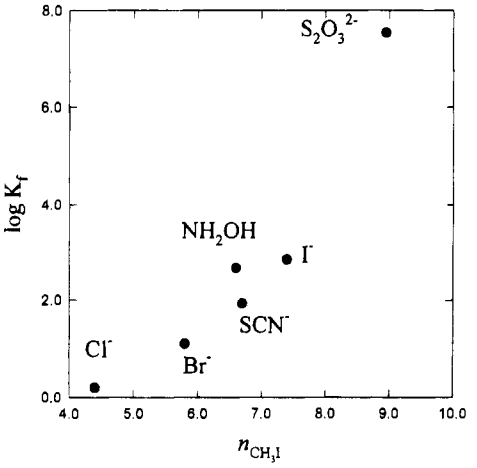

Figure 6. Dependence of the stability constants (K_f) of I_2 adducts in aqueous solution (25.0 °C) on the nucleophilic reactivity constant[37] of Lewis bases.

kinetically determined value of 480 M^{-1} for the K_f value of I_2NH_2OH. There is a great deal of scatter for the correlation in Figure 6, but it can be seen that strong adduct formation is to be expected between I_2 and NH_2OH. Hydroxylamine nucleophilic interactions are enhanced by the α effect,[38,39] added reactivity due to the presence of an unshared pair of electrons on the atom α to the donor atom. The Brønsted basicities of HPO_4^{2-} and NH_2OH are similar, but NH_2OH is a much stronger Lewis base and we find no evidence of adduct formation between HPO_4^{2-} and I_2. This is consistent with our assignment of I_2NH_2OH as the intermediate as opposed to $NH_2OI_2^-$.[8]

Summary. Iodine oxidation of hydroxylamine has a complex rate expression that is first order in $[I_2]_T$ with suppression by $[I^-]$, $[I^-]^2$, $[H^+]$, $[H^+]^2$, and [HOAc] and with acceleration by $[NH_2OH]$, $[NH_2OH]^2$, $[OAc^-]$, $[HPO_4^{2-}]$, and $[OH^-]$. Despite its complexity, this rate dependence corresponds to a straightforward mechanism (eqs 7−13) with an I_2NH_2OH adduct that reacts by general-base assistance to form INHOH as a steady-state intermediate. The decomposition of INHOH gives nitrosyl hydride (HNO) which undergoes rapid dehydrative dimerization to give N_2O. The equilibrium and rate constants for eqs 7−13 are summarized in Table 5 and give excellent fits of the data over an enormous range (4×10^7-fold) of observed first-order rate constants. The ability to fit the complex rate dependence under all these conditions lends strong support to the validity of the mechanism. The overall process corresponds to an I^+ transfer to nitrogen followed by I^- loss from nitrogen to increase the oxidation state from N(−I) to N(+I). A recent study[13] of electron-transfer reactions for the NH_2OH/NH_2OH^+ redox couple gives an estimated self-exchange rate constant of 5×10^{-13} M^{-1} s^{-1} and a giant reorganizational energy for this couple. Therefore, electron-transfer rates will be very slow. This is consistent with our evidence that ion-transfer reactions occur rather than electron-transfer reaction.

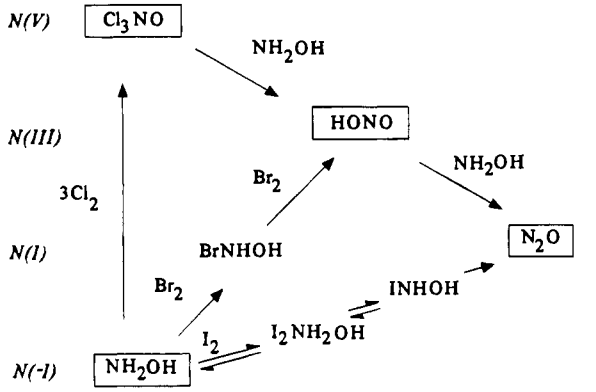

Figure 7. Different initial products of halogen oxidation of hydroxylamine. Three Cl_2 react in rapid succession to give a N(V) species that is subsequently reduced by excess NH_2OH, first to N(III) and then to N(I). Two Br_2 react in rapid succession to give N(III) before a slower reduction gives N(I). One I_2 reacts to give N(I) with kinetic evidence for I_2NH_2OH and INHOH intermediates. In the presence of excess NH_2OH the final product is N_2O for all three halogens.

Comparison of Halogen Oxidations of Hydroxylamine. The Cl_2 reactions were studied[4] from p[H^+] 0 to 1, and a rate constant of 1.6×10^9 M^{-1} s^{-1} was found for the first step in the reaction between Cl_2 and NH_2OH. A ClNHOH intermediate was proposed to react rapidly with two more Cl_2 to give Cl_3NO as the first product (Figure 7). The Br_2 reactions were studied[5] from p[H^+] 0 to 6, and a rate constant of 1.8×10^9 M^{-1} s^{-1} was found for the reaction between Br_2 and NH_2OH. A BrNHOH intermediate was proposed that reacts rapidly with a second Br_2 to give HONO as the first product. The corresponding reaction between I_2 and NH_2OH to give INHOH is much slower with a rate constant (K_Ak_b) of 5.5×10^4 M^{-1} s^{-1} when it is not base-assisted. In the presence of high concentrations of phosphate buffer, the I_2 reaction with NH_2OH is several orders of magnitude faster. There is excellent kinetic evidence for the presence of appreciable concentrations of I_2NH_2OH and for the existence of INHOH as a steady-state intermediate. In excess NH_2OH the product is N_2O. As shown in Figure 7, N_2O is the eventual product for all three halogen oxidations when excess NH_2OH is present.

Acknowledgment. This work was supported by National Science Foundation Grant CHE-9024291.

IC950705F

(38) Klopman, G.; Tsuda, K.; Louis, J. B.; Davis, R. E. *Tetrahedron* **1970**, *26*, 4549−4554.
(39) England, W. B.; Kovacic, P.; Hanrahan, S. M.; Jones, M. B. *J. Org. Chem.* **1980**, *45*, 2057−2063.
(40) Urbansky, E. T.; Cooper, B. T.; Margerum, D. W. To be submitted for publication.
(41) Mesmer, R. E.; Baes, C. F. *J. Solution Chem.* **1974**, *3*, 307−321.
(42) Molina, M.; Melios, C.; Tognolli, J. O.; Luchiari, M., Jr. *J. Electroanal. Chem. Interfacial Electrochem.* **1979**, *105*, 237−246.